Helmholtz-Zentrum Dresden-Rossendorf (HZDR)

Experimental study on the advective heat flux of a heat exchanger for passive cooling of spent fuel pools by temperature anemometry grid sensor

Unger, S.; Arlit, M.; Beyer, M.; Hampel, U.;

Specialists Workshop on Advanced Instrumentation and Measurement Techniques for Experiments related to Nuclear Reactor Thermal Hydraulics and Severe Accidents

SWINTH-2019-#XXX
Livorno, Italy, 22-25 October 2019

EXPERIMENTAL STUDY ON THE HEAT FLUX OF A HEAT EXCHANGER FOR PASSIVE COOLING OF SPENT FUEL POOLS BY TEMPERATURE ANEMOMETRY GRID SENSOR

Sebastian Unger[1], Martin Arlit[1], Matthias Beyer[1] and Uwe Hampel[1,2]

[1] Helmholtz-Zentrum Dresden-Rossendorf, Institute of Fluid Dynamics, Bautzner Landstraße 400, 01328 Dresden, GERMANY
[2] Chair for Imaging Techniques in Energy and Process Engineering, Technical University Dresden, 01062 Dresden, GERMANY
(Email: s.unger@hzdr.de; m.arlit@hzdr.de, m.beyer@hzdr.de, u.hampel@hzdr.de)

ABSTRACT

In commercial nuclear power plants spent fuel assemblies are usually stored in actively cooled water pools. The continuous decay heat release represents a potential risk in case of a station black out scenario. Thus two-phase passive heat removal systems are a key technology to enhance the safety of nuclear power plants. Such systems work only by the energy provided from the heat source, e.g. by the maintenance of a natural convection cooling. A heat transfer loop using air as an unlimited heat sink consists of a primary heat exchanger in the spent fuel pool water and a secondary heat exchanger located in ambient air. Thus the measurement of the heat flux, which gets transferred from the pool to the ambient air, is an important task. If one would measure heat flux, flow rates and temperatures in many positions by help of local probes, the natural flow would get strongly disturbed. For that reason we introduce a heat flux measurement around the secondary heat exchanger located in ambient air, which applies temperature and velocity measurement by an anemometric principle.

A $6.5 m$ long flow channel with an electrical heated finned tube heat exchanger was set up at the TOPFLOW facility at HZDR. Since the tubes of a heat exchanger would be tilted in a passive heat removal system, i.e. to allow drainage of the condensed heat transfer medium, different tiled angles were adjusted to 0° (horizontal), $20°, 30°$ and $40°$. The frontal velocity was varied between $0.5\frac{m}{s}$ and $4\frac{m}{s}$ and three thermocouples were placed up- and downstream of the heat exchanger respectively. A novel Temperature Anemometry Grind Sensor (TAGS) was located downstream the heat exchanger. It consists of a wire grid with platinum resistance elements, which are placed in the small sub-channels of a flow straightener to generate laminar flow profiles. Two methods were used to calculate the heat flux: arithmetical average and weighting of the flow area. The results of velocity was compared with the average velocity measured by the volume flow control and out of the velocity and temperature the heat flux was calculated and compared with electrical supplied heat flux. The calculated average velocity measured by the TAGS corresponds well with the velocity measured by the volume flow controller up to approximately $3\frac{m}{s}$ with a maximum deviation of $\pm 5\%$, but underestimates the velocity measured by the volume flow controller at higher velocities. The heat flux was calculated by five methods, 1.) from the three thermocouples up- and downstream of the heat exchanger, 2.) from the average temperatures measured by the TAGS, 3.) from the weighted temperature measured by the TAGS, 4.) from the average temperature and velocity measured by the TAGS and 5.) from the weighted temperature and velocity measured by the TAGS. In this order the accuracy of methods increases compared to the electrical supplied heat flux. For the last method the maximum deviation was 6.5% for all tilt angles. This new measurement concept determines the heat flux without disturbing the flow in the loop.

Specialists Workshop on Advanced Instrumentation and Measurement Techniques for
Experiments related to Nuclear Reactor Thermal Hydraulics and Severe Accidents

SWINTH-2019-#XXX
Livorno, Italy, 22-25 October 2019

KEYWORDS Finned Tube Heat Exchanger, Heat Flux Measurement, Heat Transfer, Passive Decay Heat Removal, Temperature Anemometry Grid Sensor, Velocity Measurement.

1. INTRODUCTION

In nuclear power plants the storage of spent fuel assemblies in large water pools is the usual case. Thus the decay heat generated from the fuel is transferred to the water pool, which gets cooled via active cooling systems, involving pumps, heat exchangers and water as heat transfer fluid. A promising approach to enhance the reliability of nuclear power plants is passive cooling systems, which work even in case of a longer persisting station black out. Passive heat removal systems are based on sustained natural convection of the heat transfer fluid driven by the power of the heat source. In a primary heat exchanger located in the spent fuel pool, the coolant is heated. It flows to a secondary heat exchanger and there transfers the heat to the secondary side and flows back to the primary heat exchanger. At the secondary side ambient air as an unlimited heat sink is used, hence the driving temperature difference is defined by the pool water temperature and the ambient temperature. Heat flux measurement is an important task, which usually requires the measurement of flow rate and temperature in many positions by local probes. Thus the natural convection flow would get strongly disturbed and the performance reduced. Therefore we introduce a heat flux measurement around the secondary heat exchanger located in ambient air, which applies temperature and velocity measurement by an anemometric principle. This measurement may be used to assess the heat transfer from passive heat removal system.

Computational Fluid Dynamics was used by Merzari et al. [1] to simulate the natural convection in a passively cooled spent fuel pool. Heat transfer in the fuel tank was modelled by the porous medium approach. In a similar study, performed by Ye et al. [2], it was proven, that the passive cooling removes the decay heat from the spent fuel pool effectively for different cases. In a recent study of Ayhan et al. [3] the passive residual heat removal from a nuclear reactor after shutdown was investigated. The heat transfer to ambient air with finned surfaces was studied and compared to plain tubes. As fin parameters the fin thickness, the fin radius and the total fin number were changed. The optimum was found to be $5\,mm$, $90\,mm$ and 3 for fin thickness, fin radius and fin pitch respectively. Hung et al. [4] used the porous-medium model to analyse the heat transfer capability of spent fuel pools having different fuel configurations. For the fuel rods the full-core discharge and the assumption of failing external cooling systems were used. A local boiling occurred on the fuel surface for the case without external cooling for all fuel configurations. A loop-type passive residual heat removal system, with ammonia as working fluid and air as a heat sink, was experimentally investigated by Xiong et al. [5]. The influence of different parameters, such as air velocity, hot water inlet temperature and volumetric filling ratio of the heat pipe were studied. In a following study the same author applied a similar setup with water as working fluid and a tube as an evaporator, having a long length and large diameter [6]. A significant effect of the pool water temperature on the heat pipe performance was observed, followed by air velocity, air temperature and water flow rate. Basu et al. [7] performed an extensive review on single phase natural circulation loops for solar thermal and nuclear thermal hydraulic systems. Different scaling methodologies, modelling approaches as well as unconventional topics like nanofluids, natural circulation loops for marine reactors or system dynamic issues were addressed. Fuchs et al. [8] studied experimentally the effect of ambient air and spent fuel pool water temperature on the heat transfer performance of a passive cooling system. The difference between single phase and two-phase systems was analyzed. Here the single phase system operates well at high temperature differences and the two-phase systems perform better at lower temperature differences. A passive residual heat removal heat exchanger submerged in an in-containment refueling water storage tank was experimentally investigated by Lu et al. [9]. Here a C-shaped heated rod bundle was applied as a heat exchanger, the velocity distribution in the water storage tank was measured by particle image velocimetry technique and thermocouples were placed in different positions to measure

Specialists Workshop on Advanced Instrumentation and Measurement Techniques for
Experiments related to Nuclear Reactor Thermal Hydraulics and Severe Accidents

SWINTH-2019-#XXX
Livorno, Italy, 22-25 October 2019

temperature distribution. After 4000 s sub-cooled boiling appears at the rod fuel surfaces and thus the heat transfer coefficient increases. In the study heat transfer correlations were proposed to predict this scenario. Oertel et al. studied the cooling of a partially uncovered spent fuel rack due to a loss of cooling accident [10]. Two models were applied, a first model including the pool, the building atmosphere as well as the fuel rack represented as porous medium and a second model were a geometrically resolved fuel assembly and a part of the atmosphere above was simulated. The models were linked by the atmospheric boundary condition at the representative locations. It was found, that the cross flow momentum decreases from the pool center towards the wall and thus the storage of high decay heat rate fuel assemblies near the wall seems to be favorable. For the majority of the discussed articles ambient air was suggested as heat sink. To enhance the heat transfer from the heat exchanger located in air, it is common practice to extend the heat exchanger surface. Finned tube heat exchangers are the most common device in industry to extend the heat transfer surface e.g. in cooling systems for air conditioning and refrigeration, gas turbines and compressors as well as electronics cooling. Thus, Watel et al. [11] used thermography and particle image velocimetry to determine fin efficiency and flow distribution of annular circular fins. It was found, that the air flow is increased in the mid-plane between the fins, when fin spacing increases. A horizontal cylinder with round fins was experimentally and numerical investigated by Yaghoubi et al. [12]. The measured heat transfer coefficient was low and correlations for Nusselt number as a function of Rayleigh number were proposed. A 3x3 array of electrical heated vertical cylinders immersed in a large tank of water was studied by Arshad et al. [13]. The temperatures at the cylinder surfaces and in the water tank were measured and correlations for the heat transfer of the cylinders in different locations were suggested.

The present study aims to suggest a heat flux measurement system, based on the heat transfer from a secondary finned tube bundle heat exchanger located in ambient air. In case of a passive cooling system such a finned heat exchanger needs to be inclined, in order to supply the natural convection circuit. Thus a complex three-dimensional fluid flow occurs, which makes it difficult to measure heat flux. The heat flux can be determined with the energy balance determined by the mass or volume flow and the temperature difference at the inlet and outlet of the heat exchanger. Bencs et al. investigated the heat loss by forced convection by a vortex [14]. Therefore, they used Z-type Schlieren technique for the measurement of the temperature field and Particle Image Velocimetry for flow field measurement. Funatani and Fujisawa used liquid-crystal thermometry combined with stereoscopic particle imaging velocimetry [15]. For extensive parameter studies this procedures are quite complex. Idem et al. measured the temperature distribution with two grids of 20 thermocouples each, one upstream and one downstream of the heat exchanger [16]. Averaging of the 20 temperatures to one mean temperature requires an equally distributed flow profile. Otherwise the distribution of the flow over the cross section has to be taken into account.

Within this work we compare different methods for the calculation of heat $\dot{Q}$ that is transferred from the surface of an inclined finned oval tube heat exchanger to an air flow in a rectangular channel. Therefore, in addition to the thermocouple method the thermal anemometry grid sensor (TAGS) was used. The TAGS enables the measurement of gas temperature and velocity at 16 measurement points. In the paper first we describe the flow channel and the design of the finned oval tube, the TAGS and the measuring matrix. Afterwards we explain the applied methods for the calculation of $\dot{Q}$ and present and discuss the results.

2. EXPERIMENTAL SETUP AND INSTRUMENTATION

2.1. Flow Channel and Heat Exchanger

The investigated finned tube heat exchanger was fabricated by additive manufacturing as a whole. Thus the conjunction resistance between the fins and the tube became minimum. This heat exchanger was placed in the test section of a flow channel at the TOPFLOW facility at HZDR. The

finned oval tubes have a length of $254\ mm$, a major axis of $34\ mm$ and a minor axis of $16\ mm$. The tube was connected to sleeves, which were fixed in the covers of the test section by bushings at each side. Four different combinations of covers and corresponding sleeves were used to adjust the different angle positions to horizontal (0 °), 20 °, 30 ° and 40 ° as one can see in Figure 1. The fins have a thickness of $1\ mm$, a height of $44.5\ mm$ and a spacing of $11\ mm$. Stainless steel $316\ L$ with a thermal conductivity of $16.5\ \frac{W}{mK}$ was used as construction material for the tube and fins.
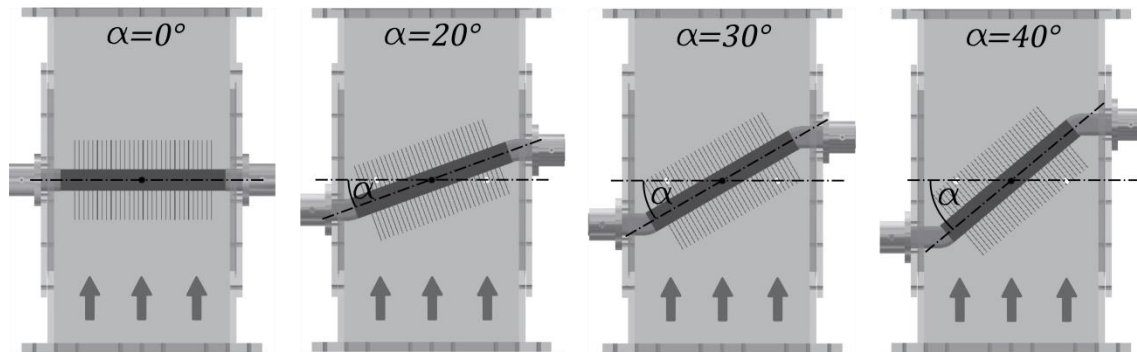

Figure 1. Different angle positions of the finned oval tube.

Inside of the oval tube three cylindrical heating rods were inserted, to apply the heating power. The gap between the rods and the inner tube surface was filled with copper power, to reduce the conductivity resistance. In order to allow a uniform heat distribution all heating rods got electrical heated parallel by a direct current power supply. A reference device (Fluke 87) was used to calibrate the power supply so the remaining uncertainty of voltage and current were $\pm 0.3\ V$ and $\pm 0.014\ A$ respectively. In fact, the accuracy calculate by error propagation of the heat input was ± 1.5 %. The experiments were performed in an flow channel made of polymethylmethacrylate with a cross-section of $270\ mm$ by $127\ mm$ and a total length of about $6.5\ m$. The manufacturing tolerances of the flow channel dimensions were measured and a deviation of $\pm 0.5\ mm$ was found. A compressor (Atlas Copco GA90+) was installed at the air inlet section of the flow channel to drive the air flow with an accuracy of $\pm 5.3\ \frac{m^3}{h}$. The volumetric flow rate was controlled by an anemometric volumetric flow controller and varied between $0.5\frac{m}{s}$ and $4.0\frac{m}{s}$. From the uncertainty of the flow channel dimensions and the volumetric flow controller an accuracy of the velocity calculated by error propagation of $\pm 0.03\ \frac{m}{s}$ was found. The volumetric flow rate and the electric heating was fixed for about $1.5\ h$ at the beginning of each campaign and further for $25\ min$ after each change of air flow rate, to ensure steady-state conditions. The heat exchanger and the instrumentation of the test section are shown in Figure 2.
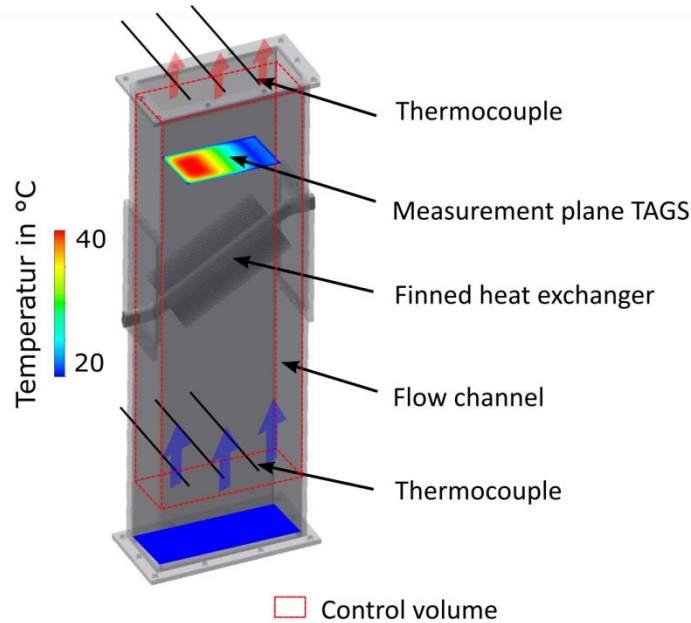
Figure 2. Test section, heat exchanger and instrumentation.

Between the flow channel inlet and the test section three sieve flow straighteners having smaller mesh size in downstream direction and a honeycomb flow straightener were installed. After steady-state was achieved all measurements were tagged for $250\ s$ with $1\ Hz$ and averaged over this time. The data recording and processing was done by a programmable logic controller, which was furthermore used to regulate the power control. Six type-K thermocouples measure the air temperature, three downstream and three upstream of the test section. These thermocouples were calibrated by a thermal calibrator (Beamex FB350) and the remaining uncertainty was $\pm 0.3\ K$. Finally, the humidity of the air flow was measured by a hygrometer (PCE-313 A), to adjust fluid properties. Right above the finned tube the thermal anemometry grid sensor was installed to measure temperature and velocity distribution, which were used to calculate the heat flux.

2.2. Thermal Anemometry Grid Sensor (TAGS)

The TAGS measures the spatial distribution of fluid temperature and velocity. For both parameters we use resistance thermometer detectors (RTD). The resistance R is a polynomial function of the sensor temperature ϑ

$$R = \frac{U_\mathrm{T}}{I_\mathrm{T}} = R_0 \cdot [1 + A_\vartheta(\vartheta - \vartheta_0) + B_\vartheta(\vartheta - \vartheta_0)^2 + higher\ order\ terms] \tag{1}$$

with the nominal resistance at reference temperature ϑ_0 and the temperature coefficients A_ϑ and B_ϑ. To avoid self-heating of the resistor the voltage U_T has to be chosen sufficient low. In the thermal equilibrium the resistor temperature is equal to the surrounding. The resistance R is calculated from U_T and the measured electrical current I_T. Applying a higher voltage U_H the resistor temperature increases by Joule heating $P_\mathrm{el} = U_\mathrm{H}/R$ and exceeds the fluid temperature. This effect is used in the thermal anemometry method for the measurement of the flow velocity. In the energy balance of the resistor

$$0 = P_\mathrm{el} - \dot{Q}_\mathrm{t} - \dot{Q}_\mathrm{c} \tag{2}$$

Specialists Workshop on Advanced Instrumentation and Measurement Techniques for Experiments related to Nuclear Reactor Thermal Hydraulics and Severe Accidents

SWINTH-2019-#XXX
Livorno, Italy, 22-25 October 2019

the heating power is in equilibrium with the total of the conductive heat flux $\dot{Q}_t$ via the resistor supports and the convective heat flux $\dot{Q}_c$. The latter is given by

$$\dot{Q}_c = \alpha(v)A(\vartheta_s - \vartheta_f). \tag{3}$$

with the heat transfer coefficient α that is a function of the flow velocity v, the surface area A of the resistor and the temperature difference $\Delta\vartheta = \vartheta_s - \vartheta_f$ between the heated resistor ϑ_s and the surrounding fluid ϑ_f.

For spatially resolved measurement we arrange 16 RTDs in an array. They are interconnected with wires from the transmitter and the receiver (Figure 3). In the referred to as temperature grid sensor (TGS) U_T is switched sequential to the transmitter wires while the others are set to ground [17] [18]. Through the RTDs in the respective row flows an electrical current whose value is measured at each receiver channel with transimpedance amplifiers. The measured temperatures are in accordance to the fluid temperatures at each RTD position. The setup for the referred to as thermal anemometry grid sensor is complemented by a voltage supply for U_H [19] [20]. One operation cycle of the TAGS has a long heating phase and a short sampling phase. In the heating phase U_H is applied to all transmitters. In the sampling phase the TAGS is operated as TGS. Now the temperatures of the heated RTDs ϑ_s are measured. The sampling phase duration has to be short compared to the thermal time constant of one RTD to avoid extensive cooling. The applied thermal anemometry operation mode is constant voltage anemometry. A constant voltage U_H is supplied to all RTDs and develops a velocity-depending thermal equilibrium state. The flow velocity is obtained from a calibration curve $v = v(\Delta\vartheta)$.
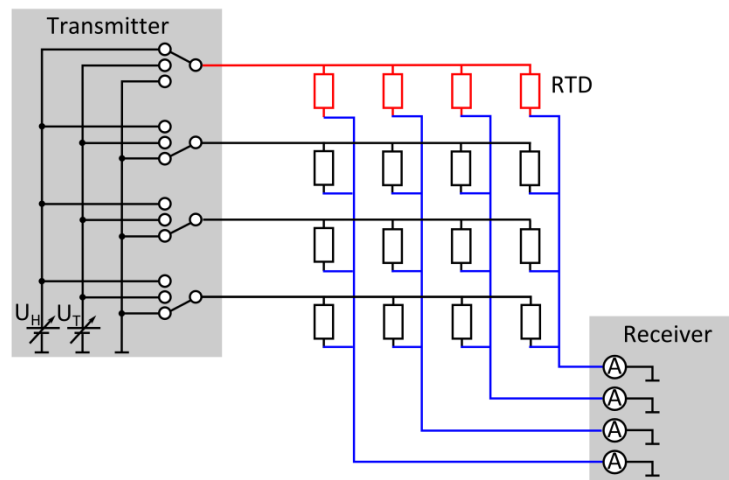
Figure 3. Circuit scheme for a combined temperature and thermal anemometry grid sensor.

The regular array arrangement is not compulsory for the actual arrangement of the measurement points in the TAGS as long as it is maintained in an electrical way. The present sensor design consists of two components: a tubular flow straightener and the TAGS measurement grid (Figure 4). Since the RTDs are sensitive to the inflow direction the upstream component is the tubular flow straightener with a diameter of $D = 2.5$ mm and a length of $L = 100$ mm for one tube. In addition to the function of forming a uniform flow the dimensions were chosen to produce a laminar flow regime in each tube. This is necessary to avoid changes in the flow regime from laminar to turbulent to ensure assignability from the measured velocity at a representative point in one tube to the average velocity. The TAGS itself is a wire grid of copper wires with a diameter of 0.3 mm (Figure 4c). The equidistant distances of the wires are 19 mm in vertical and 43 mm in horizontal direction respectively. Platinum resistors with a size of 1.6 mm x 1.2 mm x 0.65 mm are soldered at the

Specialists Workshop on Advanced Instrumentation and Measurement Techniques for
Experiments related to Nuclear Reactor Thermal Hydraulics and Severe Accidents

SWINTH-2019-#XXX
Livorno, Italy, 22-25 October 2019

crossing points of the wires whose positions are indicated by blue dots. The sensitive area of the RTDs are mounted concentrically at the end of the flow straightener tubes (Figure 4d).
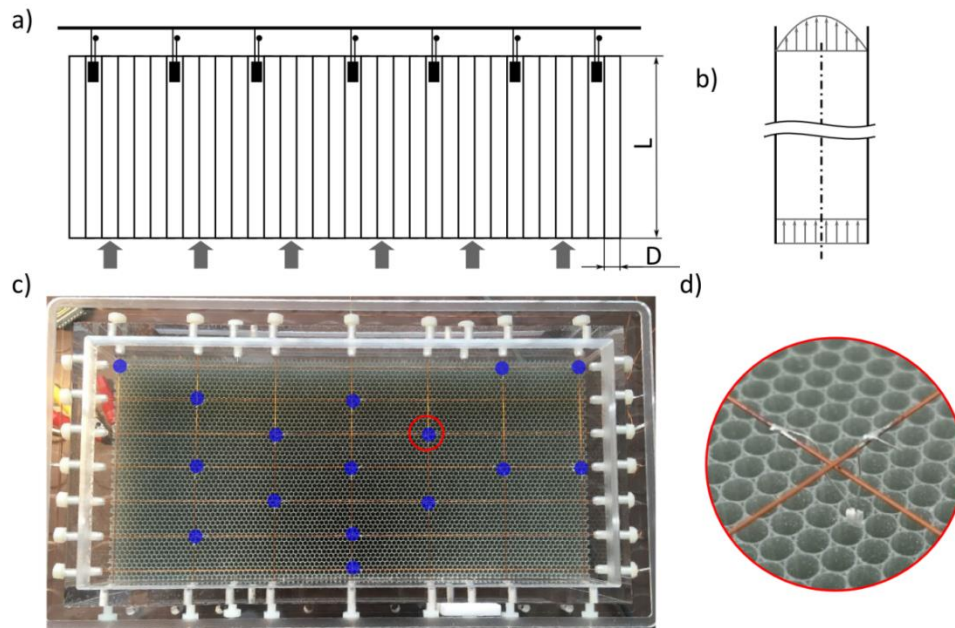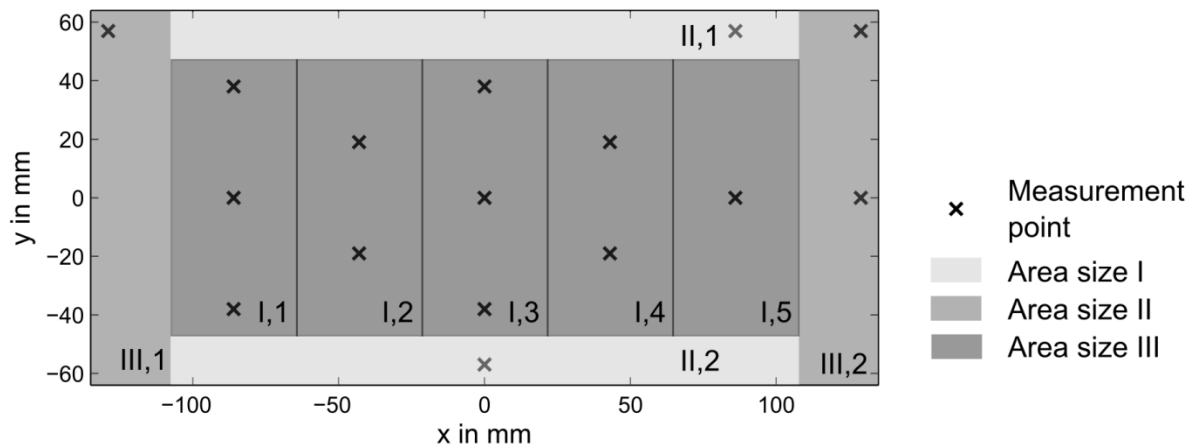

Figure 4. a) Sectional view of the sensor setup with flow straightener and TAGS b) the flow profile in one subchannel of the flow straightener c) top view photo on the sensor setup with the measurement points and d) photo of one RTD at the downstream end of one subchannel.

The whole assembled sensor was temperature calibrated. Thus, the temperature in a climate chamber was increased from 20 °C to 80 °C in steps of 5 K. The reference temperature was measured with three extra platinum resistors (class F0.1) and a precision multimeter KETHLEY 2700. Velocity calibration was performed in the flow channel without the heat exchanger. The uniformity of the flow was checked with a thermal anemometry probe (PCE-423). We found a coefficient of variation $c_v = s/\bar{v}$ of 2.4 % for an average velocity of 1.0 m/s. During calibration the average velocity was increased from 0.3 m/s to 4.1 m/s in steps of 0.3 m/s. Unfortunately, the fluid temperature decreased during the calibration procedure. Ideally, the calibration curve $v = v(\Delta\vartheta)$ is unaffected by the fluid temperature. But with the relation $\Delta\vartheta = \vartheta_s - \vartheta_f$ it is obvious that ϑ_s changes with changing ϑ_f. Thus, the heating power $P_{el} = P_{el}(R)$ varies due to $R = R(\vartheta_s)$. This means that the experimental obtained calibration curve is only valid under isothermal conditions and for ϑ_f during calibration. For universality a calibration curve transformation scheme has to be applied [21]. Summarily, the experimental calibration curve is fitted by a physical model of the heat balance around the RTD and is transformed to other fluid temperatures. The procedure is applied during calibration and the experiments.

3. DATA PROCESSING

The TAGS measurement data were averaged in both ways arithmetic and area-weighted. For the latter the channel cross-section is divided in 9 rectangular sections with different area sizes. The area size I is assigned to the sections in the middle of the cross-section, area size II to the upper and lower channel walls and area size III to the channel walls on the left and the right side. For each section a representative value is calculated from the therein located measurement points by arithmetic averaging. The weighting of one section is the proportion of its area size to the area size of the whole channel that are $A_{I,i}/A_{ges}$, $A_{II,i}/A_{ges}$ and $A_{III,i}/A_{ges}$ respectively.

Specialists Workshop on Advanced Instrumentation and Measurement Techniques for Experiments related to Nuclear Reactor Thermal Hydraulics and Severe Accidents

SWINTH-2019-#XXX
Livorno, Italy, 22-25 October 2019

Figure 5. Distribution of the measurement points in the cross-section and segmentation in sections.

For validation of the TAGS measurement results the average velocity $\bar{v}$ over the flow cross-section is compared to the average velocity v_{MFC} that results from the volume flow $\dot{V}_{\mathrm{MFC}}$ of the air supply mass flow controller. The comparability is ensured by referring to standard condition of the pressure $P = 1$ bar and the fluid temperature $\vartheta_{\mathrm{f}} = 0\,°\mathrm{C}$. Regarding to the two averaging methods $\bar{v}$ is calculated in two different ways: 1) by arithmetic averaging of the 16 velocities v_i measured with the TAGS and 2) by averaging via the area-weighting procedure (Table 1). The given velocities $v_{\mathrm{I},i} v_{\mathrm{II},i}$ and $v_{\mathrm{III},i}$ represent the average velocities measured in the associated sections $A_{\mathrm{I},i}$, $A_{\mathrm{II},i}$, $A_{\mathrm{III},i}$.

number	name	calculation
1	averaged	$\bar{v} = \dfrac{1}{16} \cdot \displaystyle\sum_{i=1}^{16} v_i$
2	weighted	$\bar{v} = \left(A_{\mathrm{I}} \cdot \displaystyle\sum_{i=1}^{5} v_{\mathrm{I},i} + A_{\mathrm{II}} \cdot \displaystyle\sum_{i=1}^{2} v_{\mathrm{II},i} + A_{\mathrm{III}} \cdot \displaystyle\sum_{i=1}^{2} v_{\mathrm{III},i} \right) / A_{\mathrm{ges}}$

Table 1. Calculation methods for the average velocity $\bar{v}$.

A general formulation of heat $\dot{Q}$ that is absorbed or dissipated by a flow passing a volume with a heat source or sink respectively is

$$\dot{Q} = \dot{m} \cdot c_{\mathrm{p}} \cdot (\vartheta_2 - \vartheta_1) \tag{4}$$

with the mass flux $\dot{m}$, the specific heat capacity of the fluid c_{p} and the temperature difference $(\vartheta_2 - \vartheta_1)$ between the outlet and the inlet in the balance area respectively. This equation is used to calculate $\dot{Q}$ in two different ways. First the influence of the temperature distribution at the outlet was studied. The adapted formulation for the heat flux is given by

$$\dot{Q} = \rho \cdot \dot{V}_{\mathrm{MFC}} \cdot c_{\mathrm{p}} \cdot (\vartheta_2 - \vartheta_1). \tag{5}$$

The mass flux $\dot{m}$ is substituted by the product of the density $\rho = \rho(p, \vartheta_1)$ and $\dot{V}_{\mathrm{MFC}}$. The inlet temperature is the arithmetic average $\vartheta_1 = \overline{\{\vartheta_{\mathrm{TC},1}; \vartheta_{\mathrm{TC},2}; \vartheta_{\mathrm{TC},3}\}}$ of the three temperatures measured with thermocouples at the inlet. Following three different methods for the determination

Specialists Workshop on Advanced Instrumentation and Measurement Techniques for
Experiments related to Nuclear Reactor Thermal Hydraulics and Severe Accidents

SWINTH-2019-#XXX
Livorno, Italy, 22-25 October 2019

of ϑ_2 are compared. In the common method #1 the outlet temperature is the arithmetic average $\vartheta_2 = \overline{\{\vartheta_{\text{TC},4};\ \vartheta_{\text{TC},5};\ \vartheta_{\text{TC},6}\}}$ of the three temperatures measured with thermocouples at the outlet. In method #2 and #3 the fluid temperature $\vartheta_{\text{TAGS},i}$ that were measured with the TAGS are used. They differ in the way of averaging, in method #2 they are averaged arithmetical and in #3 area-weighted (Table 2).

number	name	calculation
1	TC, averaged	$\vartheta_2 = \dfrac{1}{3} \cdot \displaystyle\sum_{i=4}^{6} \vartheta_{\text{TC},i}$
2	Pt100, averaged	$\vartheta_2 = \dfrac{1}{16} \cdot \displaystyle\sum_{i=1}^{16} \vartheta_{\text{TAGS},i}$
3	Pt100, weighted	$\vartheta_2 = \left(A_{\text{I}} \cdot \displaystyle\sum_{i=1}^{5} \vartheta_{\text{I},i} + A_{\text{II}} \cdot \displaystyle\sum_{i=1}^{2} \vartheta_{\text{II},i} + A_{\text{III}} \cdot \displaystyle\sum_{i=1}^{2} \vartheta_{\text{III},i} \right) / A_{\text{ges}}$

Table 2. Calculation methods for the temperature ϑ_2 at the outlet of the balance area.

In the second way first the local heat flux densities

$$\dot{q}_i = v_i \cdot \rho_i \cdot c_{\text{p}} \cdot (\vartheta_{\text{TAGS},i} - \vartheta_1) \tag{6}$$

with the flow velocities v_i and fluid temperatures $\vartheta_{\text{TAGS},i}$ are calculated. $\dot{Q}$ is obtained on the one hand side with the arithmetic average of all $\dot{q}_i$ and the cross-sectional area A_{ges} of the flow channel. On the other hand it is calculated with heat flux densities of each section $\dot{q}_{\text{I},i}$, $\dot{q}_{\text{II},i}$ and $\dot{q}_{\text{III},i}$ and its area size A_{I}, A_{II} and A_{III} respectively (Table 3).

| number	name	calculation
1	TAGS, averaged	$\dot{Q} = \dfrac{A_{\text{ges}}}{16} \cdot \displaystyle\sum_{i=1}^{16} \dot{q}_i$
2	TAGS, weighted	$\dot{Q} = A_{\text{I}} \cdot \displaystyle\sum_{i=1}^{5} \dot{q}_{\text{I},i} + A_{\text{II}} \cdot \displaystyle\sum_{i=1}^{2} \dot{q}_{\text{II},i} + A_{\text{III}} \cdot \displaystyle\sum_{i=1}^{2} \dot{q}_{\text{III},i}$

Table 3. Calculation methods for the heat flux transferred to the air flow.

4. RESULTS

4.1. Flow and Temperature Map

The measured temperature and velocity distribution is qualitatively shown in Figure 6 for the different tube inclination angles and a frontal velocity of $2\ \frac{m}{s}$. At the temperature maps one can see for the $0\,°$ orientation an area in the center, which is up to $10\ K$ higher in temperature compared to the regions nearby. With increasing inclination angle this region shifts towards one side, since the heated air, which flows in between the space of the fins gets distracted in one direction. Moreover, the temperatures are lower at the areas near the channel wall. Since the air flow partially passes through the gap between the heat exchanger, it gets not heated and remains at a lower temperature. However a higher difference between the flow velocities was not observed in the measurement plane. Furthermore there are minor differences of the velocity field, when the

Specialists Workshop on Advanced Instrumentation and Measurement Techniques for
Experiments related to Nuclear Reactor Thermal Hydraulics and Severe Accidents

SWINTH-2019-#XXX
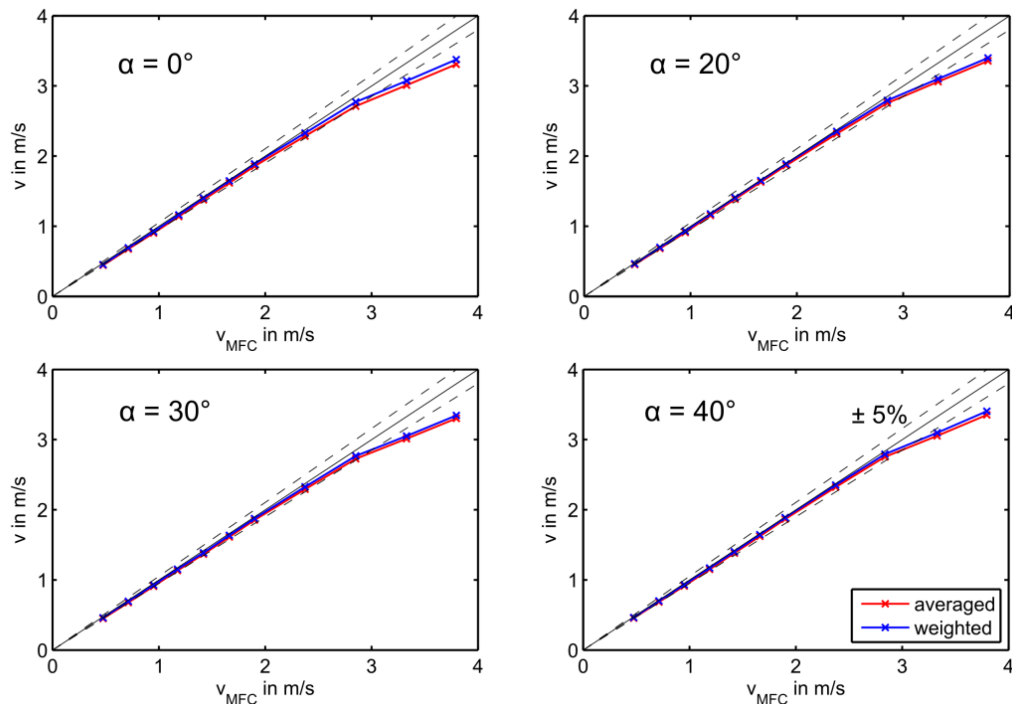Livorno, Italy, 22-25 October 2019

inclination angle changes. In fact, the velocity is evenly distributed over the cross-section with a scattering of about 8 %. A local minimum of velocity can be seen in the central area of the cross-section. This may be due to the wake region of the heat exchanger, which results in lower velocities in downstream direction. The other way around, local maxima of the velocities are on the areas near the channel walls, which may be due to bypass flows between the heat exchanger and the channel wall. However, these areas of slightly higher and lower velocities remain constant for all inclination angles.
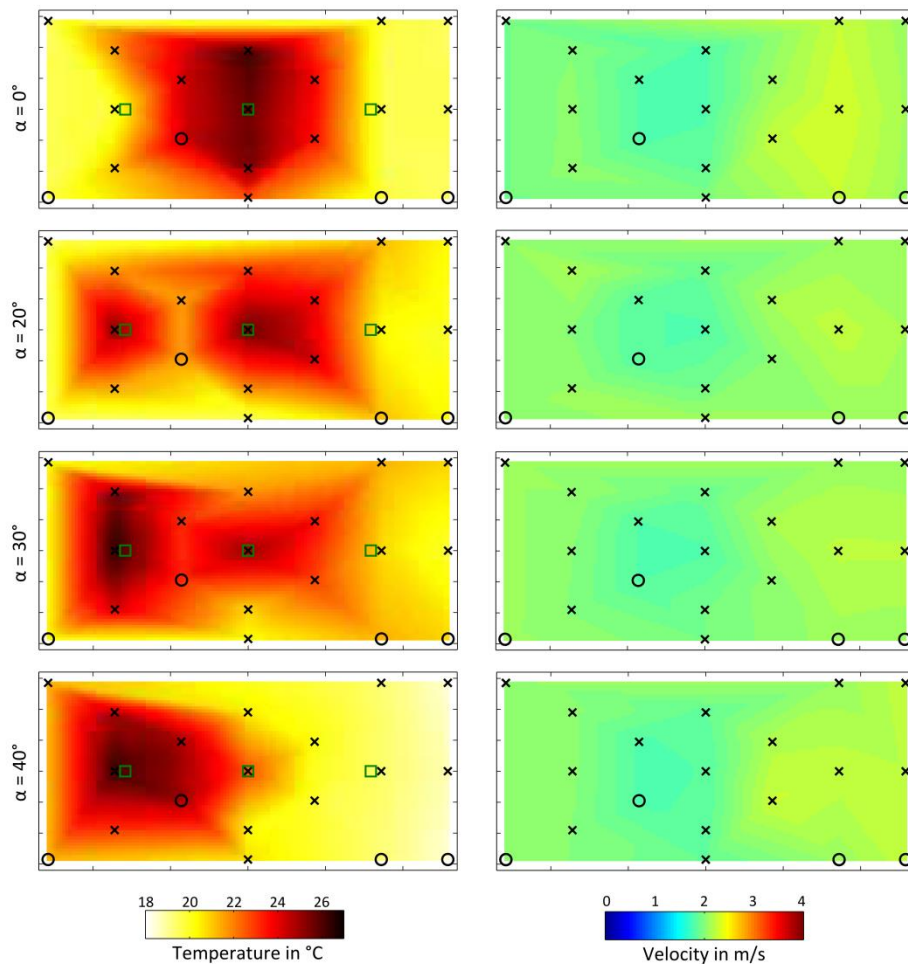
Figure 6. Temperature (left) and velocity (right) distribution map of the TAGS at different tube inclination angles and $2\ \frac{m}{s}$ frontal velocity.
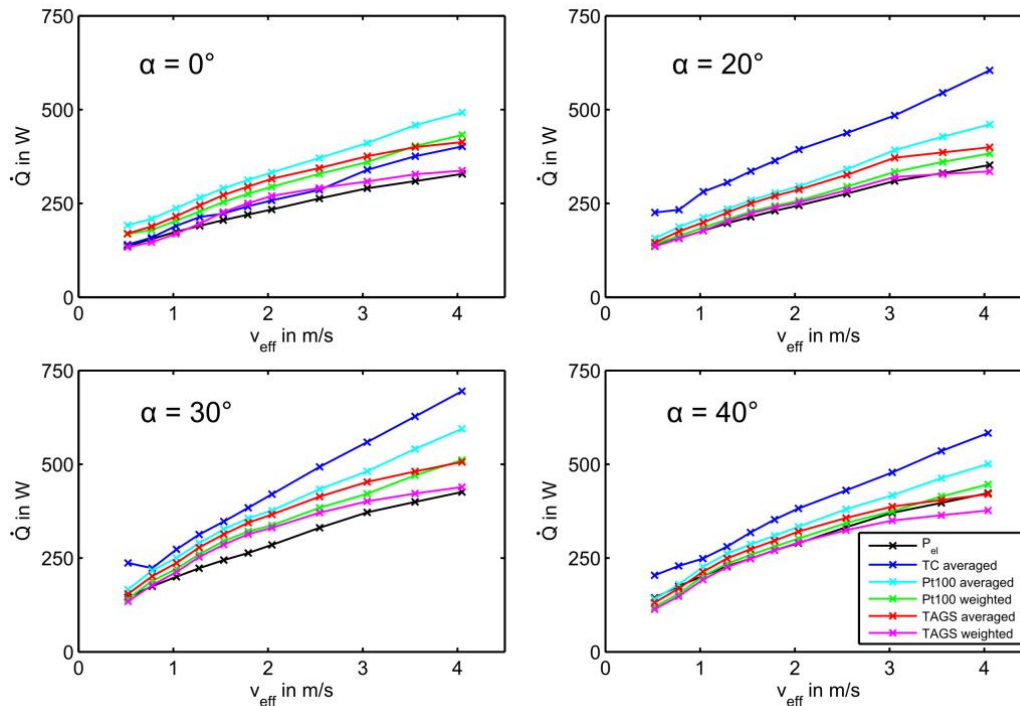
4.2. Flow Rate Validation

A comparison of the velocity measured by the anemometric volumetric flow controller v_{MFC} and the velocity calculated from the measurement of the TAGS is shown in Figure 7 for the different inclination angles. The two different methods to calculate the velocity from the TAGS measurements are included, the methods were the velocity measurements of the 16 different sensors are arithmetic averaged or averaged via the weighted areas. Until a velocity of $v_{MFC} = 2.8\ \frac{m}{s}$ both methods well represent the frontal velocity within an uncertainty of ± 5 % for all inclination angles. At a velocity of $v_{MFC} = 3.3\ \frac{m}{s}$ and $v_{MFC} = 3.8\ \frac{m}{s}$ it was underestimated by -7 % and -11 % respectively. Since this underestimation is similar for all inclination angles, a systematic measurement error is expected.

Specialists Workshop on Advanced Instrumentation and Measurement Techniques for
Experiments related to Nuclear Reactor Thermal Hydraulics and Severe Accidents

SWINTH-2019-#XXX
Livorno, Italy, 22-25 October 2019

Figure 7. Comparison of the velocity, measured with the anemometric flow measurement (v_{MFC}) and the TAGS at different inclination angles.

4.3. Heat Flux Validation

In Figure 8 the heat flux measurements from the electrical heated rods P_{el} are compared with the four different methods described in Chapter 3, where the measurements of the TAGS were used. In the first methods "TC averaged" the heat flux was calculated from the three thermocouple measurements at each of the control volume inlet and – outlet. The deviation of this method from P_{el} is high at the inclined orientations of the finned tube, which is maximum 71.7 %. However for the horizontal tube the maximum deviation is 22 %. Main reason for this high deviations is the over prediction of the temperature distribution. As one can see from Figure 6 is one thermocouple in the heated area for the horizontal orientation and two thermocouples are in the heated area for the inclined heat exchangers. However, the areas near the channel wall were not considered, since the three thermocouples are located in the middle of the cross section. Therefore we used the second methods "Pt100 averaged" and measured the temperature on the 16 different locations of the TAGS. This way we considered the temperature distribution at the cross section of the flow channel and arithmetical averaged these temperature measurements. Hence the average deviation of the heat flux compared to P_{el} reduced from 37.3 % to 26.6 % compare to the previous method. To further improve the accuracy of the heat flux measurement the measured temperatures were weighted by the area they are located as described in Chapter 3. Thus the "Pt100 weighted" heat flux values are closer to the P_{el} ones and the remaining average deviation was 12.6 %. Furthermore the deviation was similar at all inclination angles.

Specialists Workshop on Advanced Instrumentation and Measurement Techniques for Experiments related to Nuclear Reactor Thermal Hydraulics and Severe Accidents

SWINTH-2019-#XXX
Livorno, Italy, 22-25 October 2019

Figure 8. Comparison of the convective heat flux from the heat exchanger measured by the electric power supply and the TAGS at different velocities and inclination angles.

Another method is based on the determination of the heat flux at the 16 measurement locations of TAGS, which is calculated from the velocity and fluid temperature measurements. We calculated the arithmetic average of the heat flux densities q_i "TAGS averaged" and the average deviation of the different velocities and inclination angles was 18.0 % compared to the electrical heating. This way the regions with high velocity and temperature give a higher contribution to the heat flux calculation and vice versa. In fact the deviation of the "TAGS averaged" is lower compared to heat flux calculation based on the arithmetic average temperature measurements "Pt100 averaged". Finally we also weighted the heat flux measurements by the areas they are located "TAGS weighted", similar to the weighting of the temperature measurements "Pt100 weighted" earlier on. For this calculation the local heat fluxes as well as the corresponding areas are considered and the most precise results could be achieved. More precisely, an averaged deviation of 6.5 % compared to P_{el} was calculated and the measured heat flux was independently from the asymmetry of the temperature generated by the inclination angle. Therefore we recommend the last method to calculate heat flux in the most precise way. A further improvement would be possible by increasing the amount of sensors, in order to have a higher spatial resolution.

5. CONCLUSIONS

In the present study we developed and experimentally analysed a novel technique to measure the heat flux from the heat exchanger of a passive cooling system. Since these air cooled heat exchangers are usually inclined the air flow gets strongly disturbed and the heat flux measurement is a challenging task. Thus we developed a Thermal Anemometry Grid Sensor (TAGS) to measure velocity and temperature in several locations simultaneously and calculate the heat flux from these measurements. In order to validate this sensor a flow channel with a finned oval tube heat exchanger at different inclination angles of 0 °, 20 °, 30 ° and 40 ° was build up. The results of the flow velocity measurements were compared with average velocity measured by the volume flow control and a maximum deviation of ±5 % was found up to $3\frac{m}{s}$. Five different methods were used

to calculate the heat flux: 1.) temperature measurement by six thermocouples up- and downstream of the test section, 2.) average temperature measurements of the TAGS, 3.) weighted temperature measurements of the TAGS, 4.) average temperature and velocity measurements of the TAGS and 5.) weighted temperature and velocity measurements of the TAGS. Out of the applied methods the last one gave the lowest average deviation from the electrical measured heat flux of 6.5 % for all inclination angles and velocities. Thus this new measurement technique can be used to determine the heat flux from passively cooled heat exchanger with reasonable accuracy.

6. ACKNOWLEDGEMENTS

7. REFERENCES

[1] E. Merzari and Y. Gohar, "Numerical Simulation of a completely passive spent fuel pool: lessons learned," *Proceedings of the 2012 20th International Conference on Nuclear Engineering,* no. 553-561, 2012.

[2] C. Ye, M. G. Zheng, M. L. Wang, R. H. Zhang and Z. Q. Xiong, "The design and simulation of a new spent fuel pool passive cooling system," *Annals of Nuclear Energy,* vol. 58, pp. 124-131, 2013.

[3] H. Ayhan and C. Sökmen, "Investigation of passive residual heat removal system for VVERs: Effect of finned type heat exchanger tubes," *Applied Thermal Engineering,* vol. 108, pp. 466-474, 2016.

[4] T.-C. Hung, V. K. Dhir, B.-S. Pei, Y.-S. Chen and F. P. Tsai, "The development of three-dimentional transient CFD model for predicting cooling ability of spent fuel pool," *Applied Thermal Engineering,* vol. 50, pp. 496-504, 2013.

[5] Z. Xiong, H. Gu, M. Wang and Y. Cheng, "The thermal performance of a loop-type heat pipe for passively removing residual heat from spent fuel pool," *Nuclear Engineering and Design,* vol. 280, pp. 262-268, 2014.

[6] Z. Xiong, C. Ye, M. Wang and H. Gu, "Experimental study on the sub-atmospheric loop heat pipe passive cooling system for spent fuel pool," *Progress in Nuclear Energy,* vol. 79, pp. 40-47, 2015.

[7] D. N. Basu, S. Bhattacharyya and P. K. Das, "A review of modern advances in analyses and applications of single-phase natural circulation loop in nuclear thermal hydraulics," *Nuclear Engineering and Design,* vol. 280, pp. 326-348, 2014.

[8] T. Fuchs, R. Trewin, M. Reck and L. Ornot, "Passive cooling systems for spent fuel pools," *Nuclear Engineering International,* pp. 35-37, 2015.

[9] D. Lu, Y. Zhang, X. Fu, Z. Wang, Q. Cao and Y. Yang, "Experimental investigation on natural convection heat transfer characteristics of C-shape heating rods bundle used in PRHR HX," *Annals of Nuclear Energy,* vol. 98, pp. 226-238, 2016.

[10] R. Oertel, T. Hanisch, E. Krepper, D. Lucas, F. Rüdiger and J. Fröhlich, "Two-scale CFD analysis of a spent fuel pool involving partially uncovered fuel storage racks," *Nuclear engineering and Design,* vol. 341, pp. 432-450, 2019.

[11] B. Watel, S. Harmand and B. Desmet, "Influence of flow velocity and fin spacing on the forced convection heat transfer from an annular-finned tube," *The Japan Society of Mechanical Engineers,* vol. 42, pp. 56-64, 1999.

[12] M. Yaghoubi and M. Mahdavi, "An investiagtion of natural convection heat transfer from a horizontal cooled finend tube," *Experimental Heat transfer,* vol. 26, pp. 343-359, 2013.

[13] M. Arshad, M. H. Inayat and I. R. Chughtai, "Experimental study of natural convection heat

Specialists Workshop on Advanced Instrumentation and Measurement Techniques for
Experiments related to Nuclear Reactor Thermal Hydraulics and Severe Accidents

SWINTH-2019-#XXX
Livorno, Italy, 22-25 October 2019

transfer from an enclosed assembly of thin vertical cylinders," *Applied Thermal Engineering,* vol. 31, pp. 20-27, 2011.

[14] P. Bencs, S. Szabo and D. Oertel, "Simultaneous measurement of velocity and temperature field downstream of a heated cylinder," *Engineering Review,* vol. 34 (1), pp. 7-13, 2014.

[15] S. Funatani and N. Fujisawa, "Simultaneous measurement of temperature and three velocity components in planar cross section by liquid-crystal thermometry combined with stereoscopic particle image velocimetry," *Measurement Science and Technology,* vol. 13, p. 1197, 2002.

[16] S. Idem, A. Jacobi and V. Goldschmid, "Heat Transfer Characterization of a Finned-Tube Heat Exchanger (With and Without Condensation)," *Journal of Heat Transfer,* vol. 112(1), pp. 64-70, 2008.

[17] M. Ritterath, O. Öztürk and H. Prasser, "Thermo-resistive mesh sensors (TMS) for temperature field measurements," *Flow measurement and instrumentation,* vol. 22, pp. 343-349, 2011.

[18] T. Schäfer, M. Schubert and U. Hampel, "Temperature Grid Sensor for the Measurement of Spatial Temperature Distributions at Object Surfaces," *Sensors,* vol. 13, pp. 1593-1602, 2013.

[19] M. Arlit, E. Schleicher and U. Hampel, "Thermal Anemometry Grid Sensor," *Sensors,* vol. 17, 2017.

[20] U. Hampel, "Anordnung zur zweidimensionalen Messung des Geschwindigkeitsfeldes in Strömungen". Patent DE102007019927, 2008.

[21] M. Arlit, C. Partmann and E. Schleicher, "Instrumentation for experiments on a fuel element mock-up for the study of thermal hydraulics for loss of cooling or coolant scenarios in spent fuel pools," *Nuclear Engineering and Design,* vol. 336, pp. 105-111, 2018.